

# Magnetic Field Dependent Amide $^{15}\text{N}$ Chemical Shifts in a Protein–DNA Complex Resulting from Magnetic Ordering in Solution

Marcel Ottiger,<sup>‡</sup> Nico Tjandra,<sup>†</sup> and Ad Bax<sup>\*,‡</sup>

*Contribution from the Laboratory of Chemical Physics, Building 5, National Institute of Diabetes and Digestive and Kidney Diseases and the Laboratory of Biophysical Chemistry, Building 3, National Heart, Lung, and Blood Institute, National Institutes of Health, Bethesda, Maryland 20892-0520*

Received May 20, 1997. Revised Manuscript Received August 8, 1997<sup>§</sup>

**Abstract:** In solution, the degree of molecular alignment with the static magnetic field is proportional to the product of the anisotropy of the molecular magnetic susceptibility and the square of the magnetic field strength. As a result, the observed chemical shifts vary with the strength of the magnetic field and depend on the orientation of the chemical shift tensors relative to the molecule's magnetic susceptibility tensor. For protein backbone amide  $^{15}\text{N}$  nuclei in the complex between the zinc-finger DNA-binding domain of GATA-1 and a 16-bp synthetic DNA fragment, the observed field dependence of the  $^{15}\text{N}$  shifts correlates well with the dipolar couplings previously reported for this complex. This comparison indicates that, in the approximation of an axially symmetric  $^{15}\text{N}$  shift tensor, the unique axis of the  $^{15}\text{N}$  CSA tensor makes an angle of  $13 \pm 5^\circ$  with the N–H bond vector, and has a magnitude of  $168 \pm 20$  ppm. Magnetic field dependent  $^{15}\text{N}$  chemical shifts correlate well with the structure of the protein–DNA complex refined with  $^1\text{H}$ – $^{15}\text{N}$  and  $^{13}\text{C}^\alpha$ – $^1\text{H}^\alpha$  dipolar coupling constraints, but poorly with the original structure of this complex, despite relatively small rms differences between the two ensembles of structures. Magnetic field dependent chemical shifts therefore are potentially quite useful as constraints in macromolecular structure determination.

## Introduction

In solution NMR, molecules with an anisotropic magnetic susceptibility will align with the static magnetic field to an extent that is proportional to the magnitude of the susceptibility anisotropy and the square of the magnetic field strength,  $B_0$ . As a result, dipolar couplings have a residual, non-zero value, and chemical shifts (in ppm) depend on  $B_0$ .<sup>1–3</sup> Typically these effects are very small, but nonetheless, measurements of residual dipolar couplings recently have been reported for three different proteins<sup>4–7</sup> and for a double stranded DNA fragment.<sup>8</sup> The utility of these dipolar couplings for structure determination also has been demonstrated.<sup>7</sup>

Magnetic alignment also results in incomplete averaging of the chemical shift anisotropy (CSA) component of the Hamiltonian. Although field dependence of chemical shifts therefore has been predicted to be observable in solution,<sup>2</sup> to the best of our knowledge all attempts to measure such effects have failed. The main difficulty is that these effects tend to be very small, and that they are easily masked by much larger changes in

chemical shift arising from minute differences in sample temperature during the different measurements.

In the solid state, magnetic-field-dependent chemical shifts previously have been observed.<sup>9,10</sup> However, the physical basis for this effect is entirely different and relates to the fact that at low magnetic field the effective local field is not collinear with the applied magnetic field. Thus, this effect is somewhat analogous to the origin of dynamic frequency shifts<sup>11</sup> and bears no relation to the cause of the magnetic field dependence discussed in this paper.

In solution, residual dipolar couplings and field-dependent chemical shifts are reporters of the relative orientation of the corresponding tensors relative to the molecule's magnetic susceptibility tensor. In contrast to NOEs or  $J$  couplings, they therefore yield constraints which are not strictly local in nature. As dipolar couplings and field-dependent chemical shifts define the relative orientations of structural elements that are not in immediate contact with one another, they are particularly powerful complements to NOEs and  $J$  couplings. In the solid phase, where NOEs and  $J$  couplings cannot be measured, it has been proposed that dipolar and CSA information alone may even be sufficiently constraining to permit determination of polypeptide structures.<sup>12</sup> A recent study of  $^{15}\text{N}$  chemical shift anisotropy in oriented bilayers of gramicidin-A confirms that the  $^{15}\text{N}$  chemical shift information translates into tight structural constraints.<sup>13</sup>

<sup>‡</sup> Laboratory of Chemical Physics.

<sup>†</sup> Laboratory of Biophysical Chemistry.

<sup>§</sup> Abstract published in *Advance ACS Abstracts*, October 1, 1997.

(1) Gayathri, C.; Bothner-By, A. A.; van Zijl, P. C. M.; MacLean, C. *Chem. Phys. Lett.* **1982**, 87, 192–196.

(2) Bothner-By, A. A. *Encyclopedia of Nuclear Magnetic Resonance*; Grant, D. M., Harris, R. K., Eds.; Wiley: Chichester, 1995; pp 2932–2938.

(3) Sanders, C. R.; Hare, B. J.; Howard, K. P.; Prestegard, J. H. *Prog. Nucl. Magn. Reson. Spectrosc.* **1994**, 26, 421–444.

(4) Tolman, J. R.; Flanagan, J. M.; Kennedy, M. A.; Prestegard, J. H. *Proc. Natl. Acad. Sci. U.S.A.* **1995**, 92, 9279–9283.

(5) Tjandra, N.; Grzesiek, S.; Bax, A. *J. Am. Chem. Soc.* **1996**, 118, 6264–6272.

(6) Tjandra, N.; Bax, A. *J. Magn. Reson.* **1997**, 124, 512–515.

(7) Tjandra, N.; Omichinski, J. G.; Gronenborn, A. M.; Clore, G. M.; Bax, A. *Nat. Struct. Biol.* **1997**, 4, 732–738.

(8) Kung, H. C.; Wang, K. Y.; Goljer, I.; Bolton, P. H. *J. Magn. Reson. Ser. B* **1995**, 109, 323–325.

(9) VanderHart, D. L. *J. Chem. Phys.* **1986**, 84, 1196–1205.

(10) Augustine, M. P.; Zilm, K. W.; Zax, D. B. *J. Chem. Phys.* **1993**, 98, 9432–9443.

(11) Werbelow, L. G. *Encyclopedia of Nuclear Magnetic Resonance*; Grant, D. M., Harris, R. K., Eds.; Wiley: Chichester, 1995; pp 1776–1783.

(12) Cross, T. A.; Opella, S. J. *Curr. Opin. Struct. Biol.* **1994**, 4, 574–581.

(13) Mai, W.; Hu, W.; Wang, C.; Cross, T. A. *Protein Sci.* **1993**, 2, 532–542.

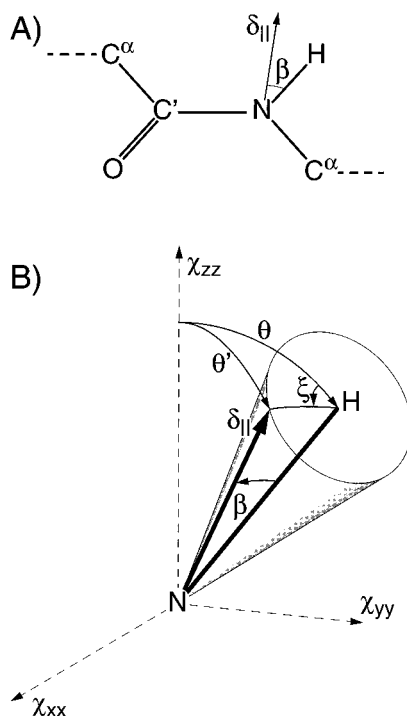


**Figure 1.** The orientation of the least shielded axis of the  $^{15}\text{N}$  CSA tensor,  $\delta_{\parallel}$ , (A) in the peptide plane and (B) in the protein's magnetic susceptibility frame with respect to the N–H bond vector.

The chemical shift tensor of peptide  $^{15}\text{N}$  nuclei is frequently assumed to be axially symmetric, with its unique axis located in the peptide plane and making a small angle,  $\beta \approx 12\text{--}24^\circ$ , with the N–H bond vector,<sup>13–18</sup> i.e. nearly orthogonal to the peptide bond (Figure 1A). Correlation of the  $^{15}\text{N}$ – $^1\text{H}$  dipolar couplings with the field dependence of the  $^{15}\text{N}$  chemical shift therefore provides information on both the magnitude of the CSA and the angle  $\beta$ . Although these two parameters cannot be separated if data are obtained for only a single backbone amide, it will be shown that reasonably tight limits can be imposed when considering the total ensemble of backbone amides.

In this study, we report the first observation of magnetic field dependence of chemical shifts in solution. We show that the observed  $^{15}\text{N}$  chemical shift changes in a protein–DNA complex are in good agreement with those expected on the basis of previously measured dipolar couplings. Chemical shift changes also are in much better agreement with a refined structure, recently calculated for this complex by the additional use of dipolar coupling constraints,<sup>7</sup> than with the original solution structure.<sup>19</sup> This suggests that field-dependent chemical shifts themselves can also be used as valuable structural constraints.

## Materials and Methods

Unless stated otherwise, NMR experiments were carried out at 37 °C on a 2 mM sample of the DNA binding domain of uniformly  $^{15}\text{N}$ -enriched chicken GATA-1, complexed with a 16-basepair synthetic

(14) Harbison, G. S.; Jelinski, L. W.; Stark, R. E.; Torchia, D. A.; Herzfeld, J.; Griffin, R. G. *J. Magn. Reson.* **1984**, *60*, 79–82.

(15) Oas, T. G.; Hartzell, C. J.; Dahlquist, F. W.; Drobny, G. P. *J. Am. Chem. Soc.* **1987**, *109*, 5962–5966.

(16) Hartzell, C. J.; Whitfield, M.; Oas, T. G.; Drobny, G. P. *J. Am. Chem. Soc.* **1987**, *109*, 5966–5969. Hartzell, C. J.; Pratum, T. K.; Drobny, G. P. *J. Chem. Phys.* **1987**, *87*, 4324–4331.

(17) Hiyma, Y.; Niu, C.-H.; Silverton, J. V.; Bavoso, A.; Torchia, D. *J. Am. Chem. Soc.* **1988**, *110*, 2378–2383.

(18) Lumsden, M. D.; Wasylisen, R. E.; Eichele, K.; Schindler, M.; Penner, G. H.; Power, W. P.; Curtis, R. D. *J. Am. Chem. Soc.* **1994**, *116*, 1403–1413.

DNA duplex, in 95%  $\text{H}_2\text{O}$ /5%  $\text{D}_2\text{O}$  (pH 6.6). The sample was purified and prepared as described elsewhere.<sup>19</sup> Spectra were recorded on Bruker DMX spectrometers, equipped with triple resonance, three-axis pulsed field gradient probeheads, operating at  $^1\text{H}$  frequencies of 750, 600, and 500 MHz. Spectra were processed with the NMRPipe software package<sup>20</sup> and peak positions were determined by contour averaging with the program PIPP,<sup>21</sup> as described previously.<sup>22</sup> Resonance assignments were taken from ref 19. To obtain estimates for the random error in each of the measurements, all spectra were recorded at least twice.

[ $^{15}\text{N}$ ,  $^1\text{H}$ ] HSQC<sup>23</sup> spectra, including a WATERGATE element for efficient water suppression,<sup>24</sup> were used for the determination of  $^{15}\text{N}$  and  $^1\text{H}$  chemical shifts. At 750 MHz, the NMR experiments were recorded as 2D data matrices of  $400^*\times 1024^*$  complex points ( $n^*$  denotes  $n$  complex points) with acquisition times of 176 ( $t_1$ ,  $^{15}\text{N}$ ) and 97.5 ms ( $t_2$ ,  $^1\text{H}$ ). At 600 MHz, data matrices were  $320^*\times 768^*$  complex points with acquisition times of 176 ( $t_1$ ,  $^{15}\text{N}$ ) and 91.6 ms ( $t_2$ ,  $^1\text{H}$ ), and at 500 MHz  $256^*\times 512^*$  complex points with acquisition times of 169 ( $t_1$ ,  $^{15}\text{N}$ ) and 78.7 ms ( $t_2$ ,  $^1\text{H}$ ). The measuring times were between 4.5 and 3.5 h per 2D spectrum. All acquired data were apodized with a 54°-shifted squared sine-bell in the  $t_2$  dimension, truncated at 1% ( $\sin^2 175^\circ$ ) at the end of the FID, and with a 54°-shifted sine-bell in the  $t_1$  dimension, truncated at 16% ( $\sin 171^\circ$ ). Data were extensively zero filled prior to Fourier transformation to yield a digital resolution of 0.55 ( $F_1$ ) and 1.3 Hz ( $F_2$ ) at 750 MHz, 0.44 ( $F_1$ ) and 1.0 Hz ( $F_2$ ) at 600 MHz, and 0.74 ( $F_1$ ) and 0.80 Hz ( $F_2$ ) at 500 MHz.

All data analysis was carried out with the program MATHEMATICA (Wolfram Inc., Champaign, IL).

## Results and Discussion

**Magnetic Alignment.** A molecule's magnetic susceptibility tensor,  $\chi$ , can be decomposed into the sum of an isotropic component,  $\chi_0$ , and an anisotropic, traceless tensor,  $\Delta\chi$ . In diamagnetic proteins,  $\Delta\chi$  is dominated by the aromatic ring systems of Phe, Tyr, Trp, and His residues, and also contains small contributions from the susceptibility anisotropies of the peptide bonds. Since the magnetic susceptibility anisotropy tensors of these individual contributors are generally not collinear, the net value of  $\Delta\chi$  in diamagnetic proteins is usually small. Much larger values for  $\Delta\chi$ , however, are obtained if many aromatic groups are stacked in such a way that their magnetic susceptibility contributions are additive, such as found in B-form DNA.<sup>8</sup> For a protein–DNA complex,  $\Delta\chi$  is therefore dominated by the DNA and to a good approximation will be axially symmetric, i.e.,  $\chi_{xx} = \chi_{yy}$ , and  $\Delta\chi = \chi_{zz} - (\chi_{xx} + \chi_{yy})/2 = \chi_{\parallel} - \chi_{\perp}$ . In this case, the magnetic-field-dependent contributions to the  $^1\text{J}_{\text{NH}}$  splitting ( $\Delta J$ ) and to the  $^{15}\text{N}$  or  $^1\text{H}$  chemical shift ( $\Delta\delta$ ) are given by:<sup>2,3,5</sup>

$$\Delta J = \text{DFS1}(B_0) - A(B_0) P_2(\cos \theta) D \quad (1a)$$

$$\Delta\delta = \text{DFS2}(B_0) + A(B_0) P_2(\cos \theta') \left(\frac{2}{3}\right) C \quad (1b)$$

where  $A(B_0) = S \Delta\chi (B_0^2/15kT)(4\pi/\mu_0)$  corresponds to the degree of magnetic alignment scaled by the generalized order parameter for internal motions,  $S$ .<sup>5,25,26</sup>  $D$  is the dipolar coupling

(19) Omichinski, J. G.; Clore, G. M.; Schaad, O.; Felsenfeld, G.; Trainor, C.; Appella, E.; Stahl, S. J.; Gronenborn, A. M. *Science* **1993**, *261*, 438–446.

(20) Delaglio, F.; Grzesiek, S.; Vuister, G. W.; Zhu, G.; Pfeifer, J.; Bax, A. *J. Biomol. NMR* **1995**, *6*, 277–293.

(21) Garrett, D. S.; Powers, R.; Gronenborn, A. M.; Clore, G. M. *J. Magn. Reson.* **1991**, *95*, 214–220.

(22) Wang, A. C.; Bax, A. *J. Am. Chem. Soc.* **1996**, *118*, 2483–2494.

(23) Bodenhausen, G.; Ruben, D. J. *Chem. Phys. Lett.* **1980**, *69*, 185–189.

(24) Piotto, M.; Saudek, V.; Sklenár, V. *J. Biomol. NMR* **1992**, *2*, 661–665.

(25) Lipari, G.; Szabo, A. *J. Am. Chem. Soc.* **1982**, *104*, 4546–4558.

constant  $[D = (\mu_0/4\pi)\gamma_X\gamma_Y h/(2\pi^2 r_{XY}^3)] \approx 22.3$  kHz, for  $^{1}\text{H}$ – $^{15}\text{N}$ ], where  $\gamma_X$  and  $\gamma_Y$  are the magnetogyric ratios of nuclei X and Y, and  $r_{XY}$  is the X–Y internuclear distance, and  $C$  is the magnitude of the chemical shift anisotropy, defined as  $\delta_{||} - \delta_{\perp}$ . Further,  $P_2(\cos \theta) = (3 \cos^2 \theta - 1)/2$ , and  $\theta$  and  $\theta'$  are the angles between the unique axis of the magnetic susceptibility tensor and the X–Y vector or the unique axis of the CSA tensor, respectively (Figure 1). DFS1( $B_0$ ) and DFS2( $B_0$ ) are magnetic-field-dependent contributions to the  $J$  splitting and isotropic shift, resulting from interference between the  $^{15}\text{N}$  CSA and  $^{15}\text{N}$ – $^{1}\text{H}$  dipolar coupling mechanisms.<sup>5,11</sup> For the relatively long rotational correlation time of the complex under study and the relatively large magnetic field strengths ( $\geq 11.7$  T), the magnetic field dependence of DFS1( $B_0$ ) and DFS2( $B_0$ ) is extremely small. In this study, their values are therefore assumed to be the same for all residues.

**Measurement of Magnetic Field Dependent Chemical Shift Differences ( $\Delta\delta$ ).** Chemical shifts for  $\delta_N$  and  $\delta_{HN}$  were taken from  $[^{15}\text{N}, ^1\text{H}]$ -HSQC spectra. To achieve maximum accuracy in peak positions, relatively long acquisition times were used in both dimensions, and data were extensively zero-filled to yield high digital resolution (see Experimental Section). Each spectrum was recorded at least twice, and the pairwise root-mean-square difference (rmsd) between two successive measurements was 0.12 ppb for  $\delta_{HN}$  and 0.48 ppb for  $\delta_N$  at 750 MHz, 0.17 ppb for  $\delta_{HN}$  and 0.69 ppb for  $\delta_N$  at 600 MHz, and 0.31 ppb for  $\delta_{HN}$  and 0.86 ppb for  $\delta_N$  at 500 MHz. Only well-resolved, sharp peaks were considered, and the six C-terminal residues were not used for further analysis because  $^{15}\text{N}$  relaxation measurements have shown that these residues are highly flexible.<sup>7</sup>

As pointed out before, the magnetic field dependence of the chemical shift can be smaller than the effect of minute changes in temperature. To separate the two effects, first a very precise measurement of the temperature dependence of the chemical shifts was made by recording two sets of HSQC spectra at two slightly different temperatures: 37 and 40 °C. Assuming the change in chemical shift is linear with temperature over this narrow range, the temperature coefficients were obtained from  $\Delta x^T = (\delta_x^{37^\circ\text{C}} - \delta_x^{40^\circ\text{C}})/3$ , where  $X = ^{15}\text{N}$  or  $^1\text{H}$ . They range from 0 to  $-11$  ppb/°C for  $^1\text{H}^N$  and from 22 to  $-24$  ppb/°C for  $^{15}\text{N}$ , and all values are listed in the Supporting Information.

Although nominally the spectra at all three spectrometer frequencies (500, 600, and 750 MHz) were recorded at 37 °C, the actual difference in temperature,  $\Delta T$ , was established by finding the  $\Delta T$  value which minimizes

$$\sigma = \sum_i [\delta_{xi}^{\text{HF}} - \delta_{xi}^{\text{LF}} - (\Delta T \cdot \Delta_{xi}^T + B_X)]^2 \quad (2)$$

where the summation extends over all  $^{15}\text{N}$  or  $^1\text{H}^N$  nuclei for which accurate shifts could be measured. The adjustable constant  $B_X$  accounts for small calibration differences (in the ppb range) between the spectra. Calculation of  $\Delta T$  with eq 3 implicitly presupposes that there is no correlation between the magnetic field and temperature dependencies of the chemical shifts. The value for  $\Delta T$  is calculated separately from the sets of collected  $^1\text{H}^N$  and  $^{15}\text{N}$  shifts, yielding  $\Delta T_H$  and  $\Delta T_N$ . The two  $\Delta T$  values, obtained in this manner, are in excellent agreement with one another ( $|\Delta T_H - \Delta T_N| \leq 0.003$  °C), whereas the actual difference in sample temperature relative to the measurements conducted at 750 MHz was much larger ( $\Delta T = 0.26$  °C at 600 MHz;  $\Delta T = 0.13$  °C at 500 MHz).

(26) Tolman, J. R.; Flanagan, J. M.; Kennedy, M. A.; Prestegard, J. H. *Nature Struct. Biol.* **1997**, 4, 292–297.

The magnetic field dependence of the chemical shifts at residue  $i$ ,  $\Delta\delta_{Xi}$ , is then calculated from the difference between the measured chemical shifts at the two magnetic field strengths, after correction for the small temperature and spectrum calibration differences:

$$\Delta\delta_{Xi}^{(\text{HF-LF})} = \delta_{Xi}^{\text{HF}} - \delta_{Xi}^{\text{LF}} - (\Delta T \cdot \Delta_{Xi}^T + B_X) \quad (3)$$

where  $\delta_X^{\text{HF}}$  and  $\delta_X^{\text{LF}}$  denote the chemical shifts of nucleus X at high and low magnetic field strength, respectively. Unless indicated otherwise, HF corresponds to 17.5 T (750 MHz) and LF to 11.7 T (500 MHz); data recorded at 600 MHz serve as a useful, independent check on the accuracy of the  $\Delta\delta_{Xi}$  values. Indeed, within experimental uncertainty in  $\delta$  (see below), chemical shifts were found to change monotonically with field strength.

Besides comparison between the observed and predicted chemical shifts at 600 MHz, the reproducibility of the above-described determination of  $\Delta\delta$  was also verified by recording a complete second set of spectra at both 500 and 750 MHz, using slightly different acquisition parameters. The pairwise root-mean-square deviation between these two independent sets of  $\Delta\delta^{(750-500)}$  values was 0.20 ppb for  $\Delta\delta_{HN}$  and 0.92 ppb for  $\Delta\delta_N$ . This indicates random uncertainties of 0.14 and 0.65 ppb in the individual measurements, and 0.10 and 0.46 ppb in their averaged values, respectively. In all further analysis we used these averaged values with assumed standard errors of 0.10 and 0.46 ppb.

**Correlation of  $\Delta\delta_N$  with Residual Dipolar Couplings.** Figure 2B shows the correlation between  $\Delta\delta_N^{(750-500)}$  and the corresponding difference in  $^1\text{H}$ – $^{15}\text{N}$   $J$  splitting,  $\Delta J_{HN}^{(750-500)}$ , which is dominated by the residual dipolar coupling. Because the unique axis of the  $^{15}\text{N}$  CSA tensor (corresponding to  $\delta_{||}$ ) is not collinear with the N–H bond vector but makes an angle  $\beta$  of about 12–24° (see also Figure 1),<sup>13–18</sup> the direct comparison of  $\Delta\delta$  and  $\Delta J$  values is rendered more difficult and we therefore first discuss the influence of  $\beta$  on this correlation.

For a given angle  $\theta$  between the N–H bond vector and the unique axis of the axially symmetric molecular magnetic susceptibility tensor (corresponding to  $\chi_{zz} = \chi_{||}$ ), the possible orientations of  $\delta_{||}$  describe the surface of a cone, centered around the N–H bond, with a semi-angle  $\beta$  (Figure 1B). The value of  $\Delta\delta_N$  depends on the angle  $\theta'$  between the  $\chi_{||}$  axis of the magnetic susceptibility tensor and the  $\delta_{||}$  axis, which ranges from  $|\theta - \beta|$  to  $\theta + \beta$ . The dashed lines in Figure 2A mark the upper and lower limits of  $P_2(\cos \theta')$  values as a function of  $P_2(\cos \theta)$ , for  $\beta = 16^\circ$ . It is readily shown that for a uniform distribution of  $\delta_{||}$  orientations on this cone,  $\langle P_2(\cos \theta') \rangle = P_2(\cos \theta) P_2(\cos \beta)$ , and the average  $\Delta\delta_N$  value,  $\langle \Delta\delta_N \rangle$ , is then described by

$$\langle \Delta\delta_N \rangle = \text{DFS2}(B_0) + A(B_0) P_2(\cos \theta) P_2(\cos \beta) \frac{2}{3} C \quad (4)$$

Under identical experimental conditions and with eq 1a, the slope of the correlation corresponds to

$$\partial \langle \Delta\delta_N \rangle / \partial \Delta J_{NH} = -P_2(\cos \beta) \frac{2}{3} C / D \quad (5)$$

When attempting to obtain the relative magnitude of the CSA and the dipolar coupling tensor from the slope of the correlation shown in Figure 2B, another factor that must be taken into account is the fact that the dipolar coupling measurements were carried out at 25 °C, whereas  $\Delta\delta$  values are obtained at 37 °C. Thus, the molecular alignment factor,  $A(B_0)$ , in eq 1 is 4% smaller for the  $\Delta\delta$  measurement, introducing another factor of 0.96 in eq 5. Linear regression of the data presented in Figure

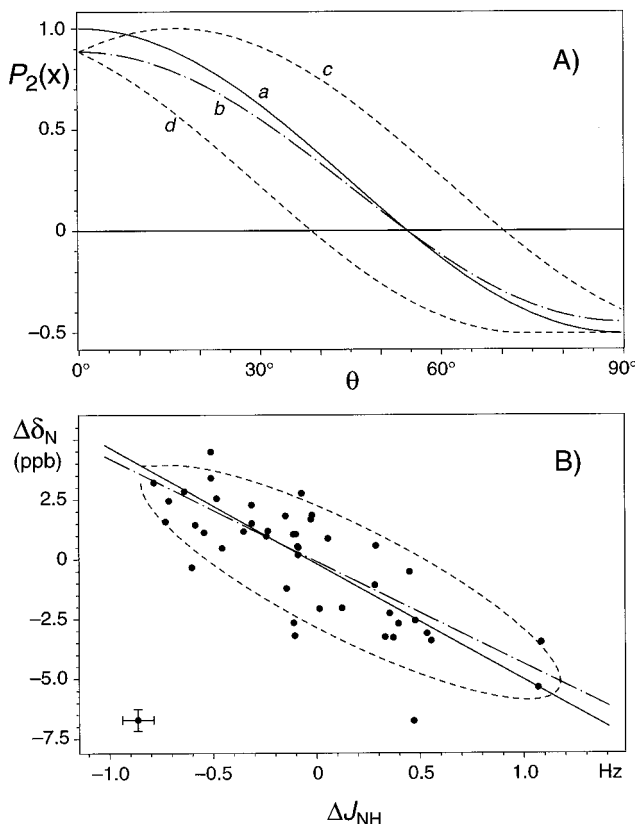


**Figure 2.** (A) Influence of the angle  $\beta$  between the N–H bond vector and the unique axis of the  $^{15}\text{N}$  CSA tensor on  $P_2(x)$  functions: a,  $P_2(\cos \theta)$ ; b,  $\langle P_2(\cos \theta') \rangle$ ; c and d, maxima and minima, respectively, of  $P_2(\cos \theta')$  for  $|\theta - \beta| \leq \theta' \leq \theta + \beta$ . (B) Plots of  $\Delta\delta_N^{(750-500)}$  versus  $\Delta J_{HN}^{(750-500)}$ .  $\Delta J_{HN}$  were taken from ref 7. Error bars are indicated in the lower left corner. The solid line corresponds to the correlation for  $\beta = 0^\circ$  and an axially symmetric  $^{15}\text{N}$  CSA of 170 ppm; the dash-dotted line corresponds to the average  $\Delta\delta_N$  expected for  $\beta = 16^\circ$ , with values distributed within the area enclosed by the dashed line. See text for further details.

2 yields a correlation coefficient  $r$  of 0.79, and assuming  $\beta = 16^\circ$ , this corresponds to a  $^{15}\text{N}$  CSA of 170 ppm.

Owing to the “random-cone” orientation of the  $\delta_{||}$  CSA axis with respect to the N–H bond vector, discrete pairs of “noise-free”  $\Delta\delta_N$  and  $\Delta J_{HN}$  values are expected to scatter around the theoretical slope, depending on the value of the angle  $\xi$  (Figure 1B). This degree of scatter is a steep function of  $\beta$ . The dashed line in Figure 2B encloses the area where  $\Delta\delta_N/\Delta J_{HN}$  pairs would be located for a uniform, axially symmetric CSA tensor with a width of 170 ppm, for  $\beta = 16^\circ$ . Considering that both the measurements of  $\Delta\delta$  and  $\Delta J$  contain considerable experimental uncertainties but most  $\Delta\delta_N/\Delta J_{HN}$  pairs fall within the area enclosed by the dashed  $\beta = 16^\circ$  line (Figure 2B), it appears that  $\beta \leq 16^\circ$ . As discussed below, correlation of measured  $\Delta\delta_N$  values with the protein structure indicates a slightly smaller  $\beta$  value of  $13 \pm 5^\circ$ .

**Correlation of  $\Delta\delta_N$  with Protein Structure.** Above, only the average value of  $\Delta\delta_N$  expected for a given  $\Delta J_{HN}$  has been considered. Because the value of the angle  $\xi$  is not taken into account, the residual error in the correlation of Figure 2B remains large. When  $\Delta\delta_N$  values are compared with values predicted by the protein’s structure, the uncertainty introduced by  $\xi$  is removed. However, now the comparison is affected by the quality of the protein structure, in addition to the assumption that all  $^{15}\text{N}$  CSA tensors are axially symmetric and of uniform magnitude. A direct correlation between  $\Delta\delta_N$  and the value of  $P_2(\cos \theta')$  in eq 1b is obtained by deriving the angle  $\theta'$  after

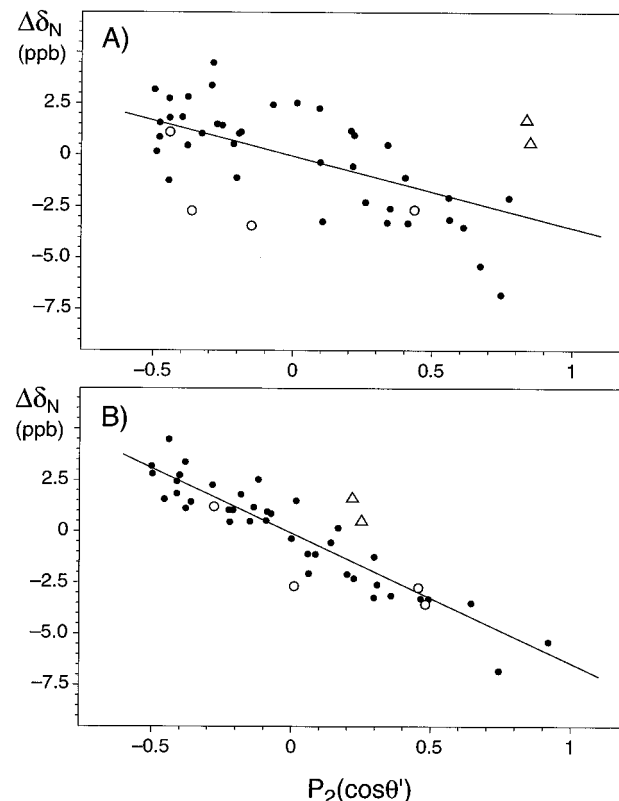


**Figure 3.** Plots of  $\Delta\delta_N^{(750-500)}$  versus  $P_2(\cos \theta')$ .  $\theta'$  angles were obtained from (A) the original NMR structure of the GATA-DNA complex<sup>19</sup> and (B) from the refined structure,<sup>7</sup> assuming  $\beta = 13^\circ$ . For part A the correlation coefficient,  $r$ , equals 0.59. For part B  $r = 0.90$ . Open circles correspond to residues 20–24 (no data were obtained for Thr<sup>22</sup> due to spectral overlap); open triangles correspond to Gly<sup>10</sup> and Leu<sup>50</sup>.

rotation of the N–H bond vector in the peptide plane by an angle  $\beta$  toward the N–C’ bond. Best linear agreement between  $\Delta\delta_N$  and  $P_2(\cos \theta')$  is obtained for  $\beta = 13.5^\circ$  (*vide infra*). The orientation of the unique axis of the magnetic susceptibility tensor which optimizes linearity of this correlation deviates by less than  $4^\circ$  from the orientation derived from  $^{15}\text{N}-^{1}\text{H}^N$  dipolar couplings.<sup>7</sup> Figure 3 shows the correlation between  $\Delta\delta_N$  and  $P_2(\cos \theta')$  for both the original<sup>19</sup> and the refined<sup>7</sup> NMR solution structures of the GATA-1/DNA complex.

For the original structure, Figure 3A shows that the correlation between  $\Delta\delta_N$  and  $P_2(\cos \theta')$  is quite poor ( $r = 0.59$ ), reflecting the relatively high uncertainty in the orientation of the peptide planes in NMR structures solved at moderate precision (root-mean-square deviation for the backbone relative to the mean coordinates is 0.76 Å), in the absence of dipolar coupling constraints. For the structure solved by the additional use of dipolar coupling constraints,<sup>7</sup> the correlation between  $\Delta\delta_N$  and  $P_2(\cos \theta')$  is much better ( $r = 0.90$ ) (Figure 3B). Although the highest correlation coefficient,  $r$ , is obtained for  $\beta = 13.5^\circ$ , the normalized error function shows that the  $\beta$  value maximizing  $r$  is rather ill defined and has a standard deviation of  $\pm 5^\circ$ .

Even in the absence of measurement error in  $\Delta\delta_N$ , and for a 100% accurate structure, considerable scatter would be expected in the correlation plot of Figure 3B, because significant deviations from axial symmetry are known to occur for the  $^{15}\text{N}$  CSA tensor.<sup>13–18</sup> Also, the magnitude of the CSA and the  $\beta$  angle are expected to vary significantly from residue to residue. The much higher degree of correlation observed in Figure 3B compared to Figure 3A reflects the higher accuracy of the structure refined by the additional use of  $^{15}\text{N}-^{1}\text{H}^N$  and  $^{13}\text{C}^{\alpha}-\text{H}^{\alpha}$  dipolar coupling constraints. It is interesting to note that

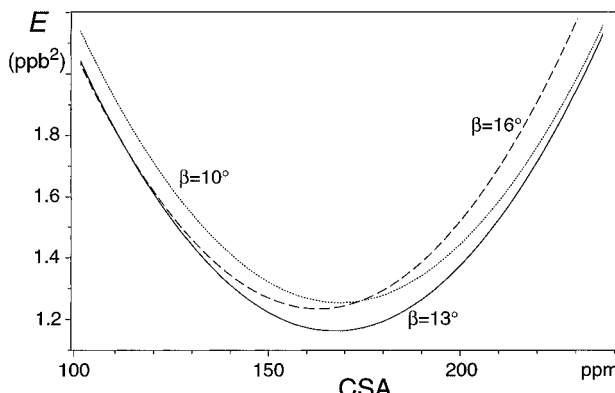


**Figure 4.** Plots of the error function  $E = \sum_i (\Delta\delta_{Ni}^{\text{pred}} - \Delta\delta_{Ni}^{\text{obs}})^2/N$  as a function of the CSA for  $\beta = 10^\circ$  (dotted line),  $13^\circ$  (solid line), and  $16^\circ$  (broken line).  $\Delta\delta_{Ni}^{\text{pred}}$  were calculated with use of eq 1b, with  $\Delta\delta = -24.4 \times 10^{-34} \text{ m}^3/\text{molecule}$  and  $S = 0.92$ .<sup>7</sup>

except for a change in the orientation of a loop, extending from residue 20 to 24 (represented by open circles in Figure 3), addition of dipolar constraints resulted only in relatively small changes in the backbone atomic coordinates. The backbone heavy atoms of residues 2–19 and 25–59 of the averaged original and refined structures superimpose to a root-mean-square deviation of 0.75 Å. Locally, however, the dipolar coupling constraints result in significant changes of peptide plane orientations relative to the average structure. The  $\Delta\delta_N$  measurements presented in this paper provide independent evidence that these changes result in a more accurate description of the average structure. For example, the open triangles in Figure 3 correspond to the backbone amides of Gly<sup>10</sup> and Leu<sup>50</sup>. The agreement between their  $\Delta\delta_N$  values and the orientations of the corresponding  $^{15}\text{N}$  CSA tensors is poor in the protein structure calculated without dipolar constraints, whereas a reasonable fit is obtained in the structure calculated with the dipolar constraints included. It is also interesting to note that the root-mean-square spread in the ensemble of refined structures relative to the mean coordinates (0.68 Å) is nearly unchanged relative to the original set of NMR structures (0.76 Å).<sup>7</sup> However, the much better agreement between the field-dependent  $^{15}\text{N}$  chemical shift information and the structures refined with dipolar constraints confirms that this latter set of structures is of considerably higher accuracy than the original set.

**Magnitude of Average  $^{15}\text{N}$  CSA.** The predicted  $\Delta\delta_N$  value is derived from the protein structure (refined by including dipolar couplings) for three different values of  $\beta$  and for a range of CSA values. The difference between the predicted and observed  $\Delta\delta_N$  values is described by the error function  $E$ :

$$E = \sum_i (\Delta\delta_{Ni}^{\text{pred}} - \Delta\delta_{Ni}^{\text{obs}})^2/N \quad (6)$$

where the summation extends over all  $N$  residues in the structured region of the protein for which  $\Delta\delta_N$  were obtained. Figure 4 plots  $E$  as a function of the magnitude of the  $^{15}\text{N}$  CSA.  $E$  is at a minimum for  $\beta = 13^\circ$  and a CSA of 168 ppm. This minimum does not depend very strongly on the assumed  $\beta$  value: for  $\beta = 10^\circ$  and  $16^\circ$ , the minimum value of  $E$  increases by ~6%, and is reached for CSA values of 169 and 163 ppm, respectively. These values are slightly higher than the value of ~160 ppm, derived from the solid state powder pattern. This discrepancy has been attributed<sup>27</sup> to the fact that solid state  $^{15}\text{N}$  CSA values usually are not scaled for the effect of fast, small-amplitude internal motions. These motions result in a 5–10%

narrowing of the solid state  $^{15}\text{N}-\text{H}$  dipolar splittings over what is expected for a static  $^{15}\text{N}-\text{H}$  pair with a 1.02-Å interatomic distance. The solid state CSA powder pattern width is therefore expected to underestimate the true CSA by the same factor. In our present study, the  $^{15}\text{N}$  CSA values in effect are scaled relative to the  $^{15}\text{N}-\text{H}$  dipolar splitting (by assuming that  $A(B_0)$  in eqs 1a and 1b has the same value). Assuming that motional averaging for the dipolar and CSA tensors is the same, the effect of internal motions on the magnitude of the average CSA cancels. The primary uncertainties in deriving the  $^{15}\text{N}$  CSA from the  $\Delta\delta_N$  values are the deviations from the assumption of an axially symmetric  $^{15}\text{N}$  CSA tensor, errors in the measured  $\Delta\delta_N$  values, and small residual errors in the refined structure. Consequently, it is not possible to derive residue-specific values for the  $^{15}\text{N}$  CSA, but only a global average.

**Effects on Amide Proton Chemical Shifts,  $\Delta\delta_{\text{HN}}$ .** The effect of magnetic field alignment on the proton chemical shifts is also examined (Table 1, Supporting Information). The changes observed in  $^1\text{H}^N$  chemical shifts are more than an order of magnitude smaller than those for  $^{15}\text{N}$  (in ppb), whereas the reproducibility of the measured field dependence, also in ppb, is only ~4 times higher. Consequently, the relative error in the field dependence of  $^1\text{H}^N$  shifts is ~3 times higher than that for  $^{15}\text{N}$ .

Values for the  $^1\text{H}^N$  CSA in the GATA-1/DNA complex have also been measured by using a recently developed scheme that is based on relaxation interference.<sup>27,28</sup> The value of the  $\text{H}^N$  CSA derived this way is based on the assumption that the  $^1\text{H}^N$  CSA tensor is axially symmetric, with its unique axis parallel to the N–H bond vector. Such measurements carried out on ubiquitin indicated that the  $^1\text{H}^N$  CSA is a strong function of hydrogen bonding and also increases with increased solvent exposure.  $^1\text{H}^N$  CSA values measured in the GATA-1/DNA complex fall in the 2–17 ppm range. These values have been used to predict the field dependence of the  $^1\text{H}^N$  chemical shifts, using the H–N bond vector orientations relative to the magnetic susceptibility tensor in the protein–DNA complex refined with dipolar constraints. Although there is substantial scatter between the measured and predicted field dependence of the  $^1\text{H}^N$  shift ( $r = 0.38$ ) (Supporting Information, Figure 1), the root-mean-square difference between the predicted and measured change is only 0.27 ppb. Although this is 2.7 times the random uncertainty in the measurement itself, it is likely that small systematic errors, such as could arise from a small, cross-correlation-induced change in the asymmetry of the  $\text{H}^N$  multiplet shape as a function of field,<sup>29</sup> could affect accurate measurement of the  $^1\text{H}^N$  shift. Also, the approximation of an axially symmetric  $\text{H}^N$  CSA tensor with the unique axis parallel to the N–H bond may be valid for protons for which a large CSA value is obtained by relaxation interference.<sup>30,31</sup> As relaxation interference only evaluates the difference between the shielding parallel to the N–H bond vector and the average shielding orthogonal to this vector, it is unlikely that the above approximation is valid when relaxation interference indicates small CSA values. The slope of the correlation between measured and predicted field dependence of the  $\text{H}^N$  shift ( $0.8 \pm 0.3$ ) is close to unity, confirming that the  $\text{H}^N$  CSA values measured previously from cross correlation roughly agree with our present measurements (Supporting Information).

(28) Tjandra, N.; Bax, A. *J. Am. Chem. Soc.* In press.

(29) Kay, L. E.; Bax, A. *J. Magn. Reson.* **1990**, 86, 110–126.

(30) Berglund, B.; Vaughan, R. W. *J. Chem. Phys.* **1980**, 73, 2037–2043.

(31) Wu, C. H.; Ramamoorthy, A.; Giersch, L. M.; Opella, S. J. *J. Am. Chem. Soc.* **1995**, 117, 6148–6149.

### Concluding Remarks

We have shown that peptide  $^{15}\text{N}$  chemical shifts in a magnetically oriented protein complex vary with magnetic field strength in a manner fully consistent with the orientation of the peptide bond relative to the magnetic susceptibility tensor of the complex. Therefore, magnetic field dependence of the  $^{15}\text{N}$  shift can be used as a powerful constraint in macromolecular structure determination, in a manner analogous to the recently proposed<sup>4</sup> and demonstrated<sup>7</sup> ability to utilize dipolar coupling constraints.

Our measurements are consistent with an axially symmetric  $^{15}\text{N}$  CSA tensor with its unique axis in the peptide plane, making an angle of  $13 \pm 5^\circ$  with the N–H bond vector and  $106 \pm 5^\circ$  with the N–C' vector. A best fit between the refined protein structure and the observed  $^{15}\text{N}$  chemical shift changes yields a  $^{15}\text{N}$  CSA value of  $168 \pm 20$  ppm. Solid state NMR analysis of short peptides<sup>14–18</sup> and of gramicidin-A<sup>13</sup> shows considerable variation in both the CSA, which ranges from 144 to 165 ppm, and  $\beta$  ranging from 12 to  $24^\circ$ . Considering that the solid state CSA values have not been corrected for rapid internal motion, our average CSA value is in excellent agreement with the solid state data.

In contrast to dipolar coupling constraints,  $^{15}\text{N}$  CSA-derived constraints are affected by the natural variations in the magnitude and orientation of this tensor relative to the peptide bond. However, resulting errors in the constraints are of similar magnitude to those from the uncertainty in the measurement itself. For example, a 20-ppm change in the  $^{15}\text{N}$  CSA from its assumed value of 168 ppm would result in an error in the CSA-derived constraint for the angle  $\theta'$ , between the CSA axis and the unique axis of the susceptibility tensor, of less than  $5^\circ$  for  $\theta'$  values in the  $25\text{--}75^\circ$  range (or  $105\text{--}155^\circ$  range).  $^{15}\text{N}$ -CSA derived constraints already have proven to be particularly useful in solid state NMR,<sup>13</sup> and results obtained in the present study indicate they can also be used in solution studies of proteins, nucleic acids, and their complexes, provided that the macromolecule has a sufficiently anisotropic magnetic susceptibility tensor.

Measurement of the magnetic field dependence of chemical shifts is in many respects simpler compared to the measurement of dipolar couplings. Chemical shift values can be obtained directly from peak-picking a simple 2D heteronuclear shift correlation spectrum, recorded at high digital resolution. It is critical, however, that the spectra are carefully phased to be

purely absorptive, as even the slightest change in phase can alter the measured position of a resonance. This requirement is frequently more difficult to meet in the detected dimension of a 2D NMR spectrum than in the indirectly detected dimension, where the required phasing parameters are easily calculated in advance<sup>32</sup> and do not require iterative adjustment. Particular attention must also be paid to correcting the effect of temperature on chemical shift. As it is difficult to have the sample temperature on different spectrometers adjusted to exactly the same value, correction for the temperature dependence of the chemical shifts must be made (*cf.* eq 2) before calculating the magnetic field dependence of the chemical shifts.

Field-dependent chemical shifts are most easily measured for nuclei with a large CSA and a high magnetogyric ratio,  $\gamma$ . From this perspective, both  $^{15}\text{N}$  and  $^1\text{H}^{\text{N}}$  are non-optimal candidates for the study of such effects. Magnetic field dependence for  $^{13}\text{C}'$  shifts, in contrast, is expected to be easier to measure; its CSA is about 25% smaller than for  $^{15}\text{N}$ , but its  $\gamma$  is 2.5 times larger and its transverse relaxation time is relatively long, yielding a narrow resonance. Although its CSA tensor is not axially symmetric, the magnitude and orientation are known to be quite uniform. Including an energetic term during structure calculation, which accounts for the difference between the observed and calculated  $^{13}\text{C}'$  field dependence, is therefore fully analogous to the previously described incorporation of dipolar constraints in the structure calculation process.<sup>7</sup>

**Acknowledgment.** We thank Frank Delaglio and Dan Garrett for assistance and use of their software, Marius Clore, Angela Gronenborn, and Dennis Torchia for many useful discussions, and James G. Omichinski for preparation of the GATA1-DNA complex. This work was supported by the AIDS Targeted Anti-Viral Program of the Office of the Director of the National Institutes of Health. M.O. is supported by a Swiss National Science Foundation postdoctoral fellowship.

**Supporting Information Available:** One table containing the chemical shifts, field dependent chemical shift differences, and temperature coefficients for  $^{15}\text{N}$  and  $^1\text{H}^{\text{N}}$  of GATA, and a plot of the measured proton chemical shift differences,  $\Delta\delta_{\text{HN}}^{\text{obs}}$ , *versus* the predicted values,  $\Delta\delta_{\text{HN}}^{\text{pred}}$  (3 pages). See any current masthead page for ordering and Internet access instructions.

JA971639E

---

(32) Bax, A.; Ikura, M.; Kay, L. E.; Zhu, G. *J. Magn. Reson.* **1991**, *91*, 174–178.